Detection and Modeling of Pedestrian Groups Using Laser Sensor Trajectories

Toshihiro Osaragi[1*], Tomona Takeuchi[2*], Hiroyuki Kaneko[3*]

[1] School of Environment and Society, Institute of Science Tokyo – osaragi.t.20f7@m.isct.ac.jp
[2] School of Environment and Society, Tokyo Institute of Technology – takeuchi.t.aj@m.titech.ac.jp
[3] Kajima Technical Research Institute, Japan – kaneko-hiroyuki@kajima.com

Keywords: pedestrian behavior model, pedestrian group, psychological stress, laser sensor trajectories.

ABSTRACT:

This study proposes a pedestrian behavior modeling framework that explicitly incorporates the existence and dynamics of pedestrian groups. Using high-resolution laser sensor data collected in a hospital atrium, spatiotemporal features describing interpersonal distance, relative speed, and walking direction are extracted from pedestrian trajectories. Based on these features, machine learning techniques are applied to identify pedestrian groups, with Support Vector Machines (SVM) and Random Forests used as baseline models. The results show that the SVM achieves stable and accurate group identification under complex walking conditions. Building on the detected group structures, the pedestrian behavior model is extended to represent group-related psychological stress, including individual stress, stress induced by other pedestrians, and stress arising from group dispersion. Model parameters are calibrated using laser-derived trajectory data with individual attributes such as staff roles and mobility aid usage. The proposed model reproduces observed walking trajectories with high fidelity, achieving position errors within 80 cm for approximately 80% of pedestrians. Finally, the model is applied to spatial evaluation of pedestrian environments by mapping distributions of estimated psychological stress. The results reveal elevated stress levels in waiting areas such as reception zones, while group dispersion stress is more prominent in low-density regions where groups tend to spread out. These findings demonstrate that incorporating pedestrian group behavior enhances the interpretability and applicability of pedestrian models for evaluating and designing public spaces.

1. Introduction

Pedestrian simulation models that accurately describe the complex dynamics of human walking behavior have long served as essential tools for planning, designing, and evaluating pedestrian spaces. Beyond simple motion reproduction, such models enable the quantitative assessment of spatial comfort, congestion, and safety.

Early theoretical foundations of pedestrian dynamics include force-based, cellular automaton, and rule-based approaches. Among them, Helbing and Molnár (1995) proposed the social force model (SFM), which has become one of the most influential frameworks for describing pedestrian interactions and evacuation dynamics. Subsequent studies extended these ideas to a wide range of pedestrian contexts, including bottleneck flow, bidirectional movement, and emergency evacuation (Schadschneider et al., 2009; Hoogendoorn and Bovy, 2004).

The analysis of coordinated pedestrian group behavior has also been explored in earlier studies. Trajectory-mining studies in the late 2000s and early 2010s investigated small-group movement, social ties, and leader–follower structures using video-based tracking and spatio-temporal clustering techniques. For example, Moussaïd et al. (2010) demonstrated that pedestrians walking in social groups exhibit distinct spatial formations and speed adaptation, while Ge et al. (2009) proposed methods for detecting pedestrian groups from trajectory data based on motion similarity and interpersonal distance. These studies highlighted the importance of group behavior in shaping local flow patterns and interaction structures.

In recent years, interest in pedestrian group detection has intensified due to the availability of large-scale, high-resolution trajectory data and advances in computational methods. Traditional clustering approaches such as k-means and DBSCAN have been applied to pedestrian group detection in trajectory-based studies (e.g., Chen et al., 2022), while more recent preprint studies employ hybrid modeling and deep learning techniques to detect dynamic pedestrian groups in real time from continuous trajectories (Sanjjamts et al., 2025). These developments have renewed attention to group-level crowd micro-dynamics in dense environments (Nicolas & Hassan, 2021).

Meanwhile, advances in sensor technology have significantly improved the precision and anonymity of pedestrian monitoring. High-resolution laser and LiDAR sensors can now capture pedestrian positions with centimeter accuracy (Xiao et. al, 2016; Borgmann et al., 2020; Na et al., 2023). Doppler LiDAR has further enabled the acquisition of both positional and velocity information, facilitating robust multi-pedestrian tracking under occlusion and cluttered conditions (Peng and Shan, 2021). These sensing advancements provide the foundation for automated group identification and the quantitative modeling of interpersonal interactions in real environments.

In parallel, there is a growing movement toward integrating psychological measures into pedestrian behavior models. Recent studies have quantified pedestrian stress using biometric sensors and self-reported surveys (Ma et al., 2025), underscoring the importance of perceptual comfort and mental load in space evaluation. Similarly, Geometric Graph Neural Network models (Honarvar and Diaz-Mercado, 2024) have demonstrated that social and spatial interactions among pedestrians can be effectively represented as graph structures, offering new potential for capturing complex inter-group dynamics.

Despite these advances, there remain two major gaps: (1) few studies have explicitly combined laser-based trajectory data with group-level behavioral modeling, and (2) psychological stress within and between pedestrian groups has seldom been

This contribution has been peer-reviewed. The double-blind peer-review was conducted on the basis of the full paper.
https://doi.org/10.5194/isprs-annals-XI-4-2026-267-2026 | © Author(s) 2026. CC BY 4.0 License.

quantified for spatial evaluation. The integration of these perspectives is crucial for accurately assessing pedestrian space performance, particularly in public facilities where both individual and collective comfort must be balanced.

Therefore, this research develops a pedestrian behavior model that explicitly incorporates group detection and psychological stress based on high-precision laser trajectory data. The objectives are as follows:

(1) to develop an automated procedure for detecting pedestrian groups from continuous trajectory data;

(2) to construct a pedestrian behavior model that represents individual psychological stress, inter-group stress, and inter-group stress; and

(3) to validate the proposed approach using laser-based pedestrian monitoring data and apply it to evaluate spatial stress distributions in real environments.

Through this approach, the proposed model aims to bridge micro-scale behavioral mechanisms with macro-scale spatial evaluation, contributing a novel analytical framework for pedestrian-centric design and assessment of architectural spaces.

2. Parameters for Detecting Pedestrian Groups

This research defines a “pedestrian group” as multiple pedestrians who are conscious of each other, enter the study area at about the same time, and proceed together toward the same destination. Some cases consist of staff members and patients temporarily moving together. An example of this is discussed below, such cases are also considered “groups”.

We now examine the spatiotemporal relationships among the walking trajectories of multiple pedestrians. Under normal circumstances, we would expect to see intrinsic special relationships in the relative distances, speeds, and angles among pedestrians who are walking together as a single group. Since these relationships can be expected to vary with the density of people surrounding the group, some parameters were defined for the spatiotemporal relationships shown in Fig. 1(a, b). These are the distance between intergroup members, their speed differences, and their relative angles. There can also be differences in these values between any two group members.

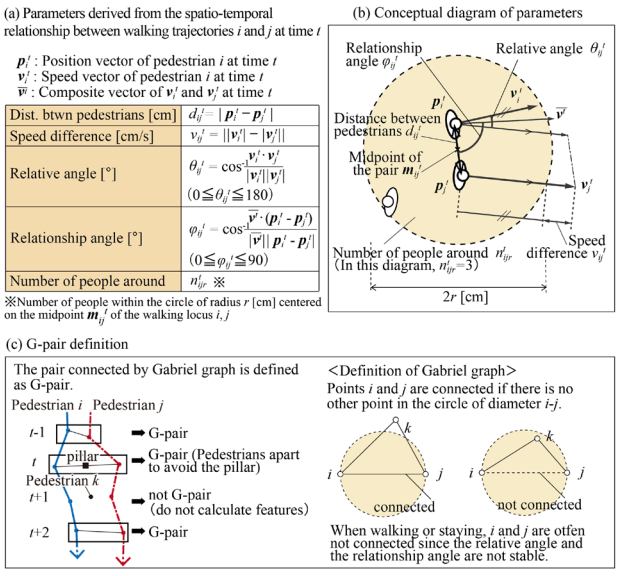

Figure 1. Parameters for pedestrian group detection.

Note that the “relationship angle” refers to the angle between the average walking directions of two pedestrians and the chord between them. The closer this value is to 90°, the more it suggests that the pair are walking in parallel. The number of nearby people was defined as the number of people within a certain circle centered at the midpoint between two pedestrians. The radius r of this circle, which was initially undetermined, was estimated during the model calibration process.

If all of the above parameters were calculated for arbitrarily selected pedestrian pairs, this process would include pedestrians who are obviously not within the same group and would result in an inefficient analysis. Therefore, a Gabriel graph was employed to efficiently define adjacency relationships between pedestrians, as shown in Fig. 1(c). To maintain computational efficiency, the parameters were calculated only for pedestrian pairs directly connected on the graph (hereafter referred to as Gabriel pairs, or G-pairs). Although each G-pair represents a dyadic relationship, groups consisting of three or more pedestrians can be represented when one or both pedestrians in a G-pair are connected to additional pedestrians through the Gabriel graph. In such cases, multi-member pedestrian groups emerge as connected subgraphs formed by multiple G-pairs.

Figure 1(c) illustrates the definitions on the Gabriel graph and provides an example of the parameter calculations for a G-pair.

3. Pedestrian Behavior Model Incorporating Pedestrian Groups

In order to develop more precise descriptions of the different behaviors of lone pedestrians and pedestrian groups, it is necessary to make some improvements to the pedestrian behavior model based on psychological stress. The route selection model and pedestrian walking model employed in this study is based on a previously proposed framework developed by Osaragi (2004) and later refined and empirically estimated using high-precision pedestrian trajectory data by Osaragi et al. (2022). For clarity and completeness, the core structure of these baseline models is briefly summarized here so that the present paper can be understood independently.

It is thought that a pedestrian (1) selects an approximate movement path that will take them efficiently to their destination, and (2) proceeds along that path, changing it in a dynamic process as appropriate for the surrounding environment, including the presence of other nearby persons. By this logic, pedestrian behavior can be modeled via two processes (Fig. 2(a)), namely (1) in which using a route selection model, the path to the destination of minimum cost is determined using a triangular irregular network (TIN), and (2) a walking model is used while the subjects are actually moving so that the sum of the psychological stress levels from the environment is minimized from moment to moment, as shown in Fig. 2(b). These are pedestrian stress (*PS*), destination stress (*DS*), and obstacle stress (*OS*). Thus, the sum of the psychological stress levels from the environment is modeled by the Eq. (1).

$$
\begin{aligned}
&Stress = PS + DS + OS \\
&where\ PS = \gamma_1 \sum_j \exp\left[-\alpha_1 d_{jp}\right] \\
&\qquad DS = \gamma_2 (d_{ep} / v_i)^{\alpha_2} \\
&\qquad OS = \gamma_3 \sum_k \exp\left[-\alpha_3 d_{kp}\right] \\
&\qquad d_{jp} = \sqrt{(d_0 \beta_1 \sin\theta)^2 + (d_0 \cos\theta)^2} \quad for\ \cos\theta \geq 0 \\
&\qquad d_{jp} = \sqrt{(d_0 \beta_1 \sin\theta)^2 + (d_0 \cos\theta / \beta^2)^2} \quad for\ \cos\theta < 0
\end{aligned}
\tag{1}
$$

Here α_1, α_2, α_3, β_1, β_2, γ_1, γ_2, γ_3 are unknown parameters, d_0 is actual distance between arbitrary position and other person j, d_{jp} is relative distance between arbitrary position and other

pedestrian *j*, d_{ep} is actual distance between arbitrary position and provisional position, d_{kp} is distance between arbitrary position and obstacle *k*, θ is angle between arbitrary position and other pedestrian *j*, and v_i is walking speed of pedestrian *i*. The reader is directed to Osaragi et al. (2022) for further detail about these models.

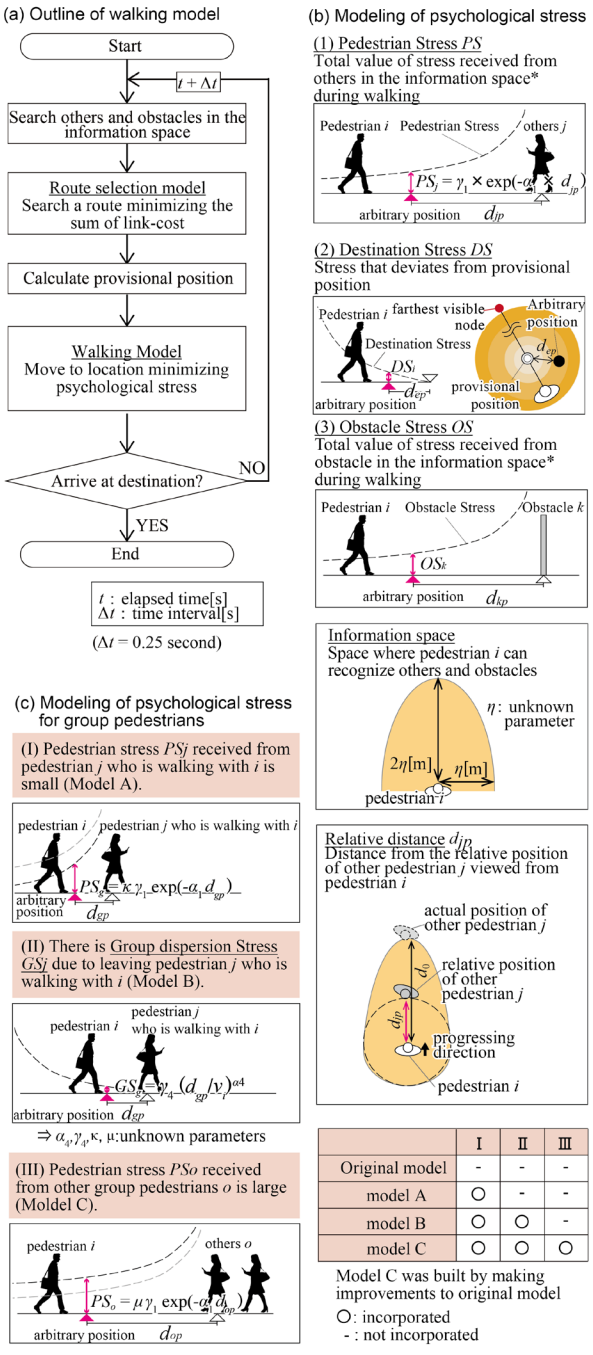

Figure 2. Pedestrian behavior model with pedestrian groups.

Improvements were made to the walking model to account for the behavior of pedestrian groups, as shown in Fig. 2(c). The PS_g produced by other members of the own group is probably less than that produced by other people present in the environment. This is called “Model A” shown in Fig. 2(c)(I). When the group dispersion stress (GS_g), defined as the stress caused by separation from the group, is added, this becomes “Model B”, which is shown in Fig. 2(c)(II). Additionally, the stress from pedestrians of the other group (PS_o) is greater than that of a lone pedestrian. This was incorporated in “Model C”, as shown in Fig. 2(c)(III). The psychological stress PS_g, GS_g, PS_o for incorporating pedestrian groups are modeled as Eq. (2) and added in Eq. (1).

$$\begin{aligned} PS_g &= \kappa\gamma_1 \exp\left[-\alpha_1 d_{gp}\right] \\ GS_g &= \gamma_4 (d_{gp} / v_i)^{\alpha_4} \\ PS_o &= \mu\gamma_1 \exp\left[-\alpha_1 d_{op}\right] \end{aligned} \tag{2}$$

Here α_4, γ_4, κ, μ are unknown parameters.

4. Survey of Pedestrian Groups in a Hospital

A wide assortment of individuals and groups of people including patients, helpers, and hospital staff walk through the atrium area of a hospital as individuals, or by forming groups, while sometimes crossing each other’s paths. A behavior monitoring survey by laser sensor was conducted in the atrium area of Hospital S in Tokyo in order to examine the characteristics of groups walking together. The positions and orientation of the LiDAR sensors are shown in the Fig. 3(a), and the arrows indicate the sensing direction of each sensor. More specifically, six laser sensors, which are excellent devices for preserving anonymity, were employed to obtain highly precise records of pedestrian trajectories. These sensors have been found to be quite useful for measurements in hospitals where privacy protection is one of the highest priorities.

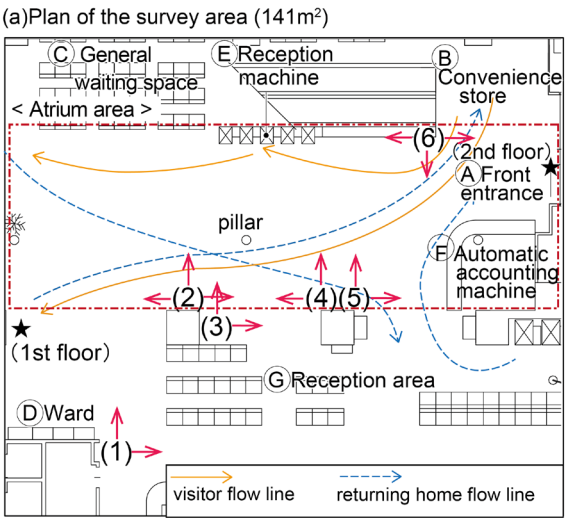

(b)Outline of the survey (Surveys 1-1 and 1-2)

Outline of Hospital S	
Number of beds	535 beds
Number of outpatients/day	1,182 (2015)
Outline of survey	
Survey1-1 (Behavior monitoring survey by laser sensor) 762 trajectories (14:30-15:30, Wed, Oct 31, 2017: Trajectory B) 800 trajectories (14:30-15:30, Thu, Nov 01, 2017: Trajectory A)	
Survey1-2 (Group survey by visual observation) time, position and attributes of the group (the same date and time as Survey 1-1)	

Figure 3. Outline of surveys (Surveys 1-1 and 1-2).

The emitted laser beams detect the torso and surface of the human body, enabling the acquisition of point clouds corresponding to individual pedestrians. For each detected

pedestrian, the centroid of the point cloud representing the human body surface was calculated and defined as the representative point of the individual. The position of this representative point was computed at 0.1-second intervals, and the resulting sequence of coordinates was used to construct pedestrian movement trajectories. Using the centroid of the body surface point cloud reduces the influence of partial occlusion and body orientation, providing a stable estimate of pedestrian position for trajectory analysis.

Figure 3(b) shows the dates and times when the observations were carried out. The data from the visiting period from 14:30 to 15:30, a time when groups are particularly numerous because of visiting inpatients or other reasons, was pre-processed and the trajectories of 762 and 800 people were extracted from the records for Oct. 31 and Nov. 1, 2017, respectively (Surveys 1-1 and 1-2). Thus, a total of 1,562 trajectories was examined (Fig. 3(b)).

In parallel with the laser measurements, two research team members visually observed the pedestrian traffic to identify groups, and they recorded the observation times, locations, and individual attributes. We adopted following standards as indicators for the visual observation team to identify a pair of pedestrians as a group. (1) The pedestrians entered the study area at about the same time; (2) they walked toward the same destination; (3) they traveled together to the return visit reception counters, bill paying machine or the like; (4) they mirrored each other in motions such as stopping or wandering; (5) they faced each other and they conversed with each other. There were also special groups that had been identified based on the subjective judgment of the observation team. However, nearly all the identified groups were easy to identify from the visual observations, and observation team members were in close agreement regarding their group identifications. The purpose of noting the times and locations was to tie the information from Survey 1-2 to the Survey 1-1 data. Then, using the analytical data for both days, they created two measured trajectory records, designated as Trajectory A and Trajectory B.

We previously (prior to the remodeling of Hospital S) carried out a nearly identical research in the atrium area of the same Hospital S. Another measured trajectory record (Trajectory C) was also recorded with all the pedestrian attributes in the visual survey. This data will be used for further analysis in the latter half of this research.

An analysis of survey data from a completely different, remodeled atrium area is conducted in this research. However, since it was the same hospital, there were no notable changes in the patient population or hospital staff before and after the remodeling. Additionally, since identical laser sensor observations were conducted, we do not believe that the changes in the surveyed space had any notable effect on our results, at least from the viewpoint of our objective, which was to investigate methods for detecting pedestrian groups.

5. Machine Learning for Group Detection

5.1 Estimation of Parameters using Observed Trajectories

We used a Support Vector Machine (SVM) and Random Forest algorithms for machine learning in an attempt to detect groups, which are available in a statistical analysis environment R. Although graph neural networks (GNN) are relevant for modeling pedestrian interactions, this study adopted relatively simple and interpretable models to ensure robustness under limited data conditions.

First, the specific values to be used for the group detection of all the trajectory pairs in Trajectories A and B, which are described below as detection parameters P1 to P5, were calculated as shown in Fig. 4(a, b). Next, group detection teaching was carried out thoroughly using Trajectory A. When that process was completed, Trajectory B was applied to the group detection model and the accuracy of the model was examined for validity.

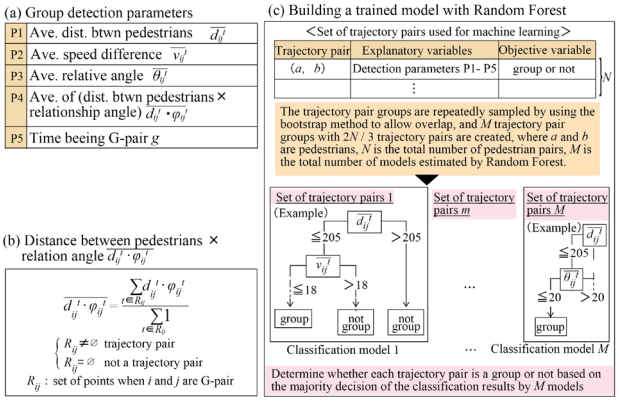

Figure 4. Group detection using machine learning.

An SVM guarantees a comprehensive optimal solution even when used for validation with unlearned walking patterns, as seen in the case of Trajectory B, which means it can provide highly accurate group detection. In contrast, the random forest algorithm is an ensemble learning procedure that is composed of numerous decision trees, as shown in Fig. 4(c). Its advantage is that it can evaluate the utility of the various group detection parameters.

Using the learned group detection model on Trajectory B, the F values for extracting groups were 86.9% and 83.1% for the SVM and random forest algorithm, respectively, thus indicating that both showed good results, as can be seen in Fig. 5(a). In terms of the F values, the SVM showed higher stability and better accuracy than the random forest algorithm both in Trajectory A learning and model validation using Trajectory B. The reader can also see that the SVM handled the measured trajectory record composed of unobserved data in a flexible way, and that the random forest algorithm scored 100% in group detection during learning. This may have been due to an issue that is called “over-learning”.

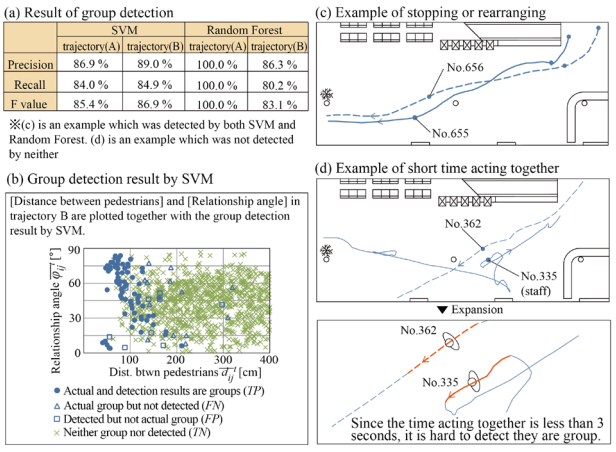

Figure 5. Validation of group detection using machine learning.

In Fig. 5(b), the reader can also see that SVM was successful in detecting groups using the complicated relationships between

the relative distance d_{ij}^t and the relationship angle θ_{ij}^t. Group pairs that stopped together or exchanged positions while walking was more difficult to identify using the thresholds, but after machine learning, they could also be detected by the SVM. For example, pedestrian Nos. 655 and 656, shown in Fig. 5(c), walked in a complicated path, switching between left and right sides repeatedly, but were still correctly detected as a group.

There were also group pairs that remained unidentified by both algorithms, and other pairs that moved detectably as a group only for periods that were too short to meet the standards, as shown in Fig. 5(d). Finely detailed behaviors exhibited by a trajectory pair such as members facing each other or talking to each other are immediately obvious group pair indicators to human observers. However, since this information cannot be captured by laser sensor observations, the collection of such detailed information, which will continue to require direct human observations, will remain necessary as we work to make meaningful advancements in group detection accuracy levels.

5.2 Evaluation of the Utility of Detection Parameters

Figure 6(a) shows the importance of the detection parameters used in the random forest method. As can be seen in P5, the number of seconds coupled on the Gabriel graph, which is shown in Fig. 4(a), is the most important parameter. Here, it can also be seen that Gabriel graphs, which were originally introduced to define adjacency relationships, provide essential information for group identification. This result is consistent with the definition of groups in the model proposed by Osaragi (2004).

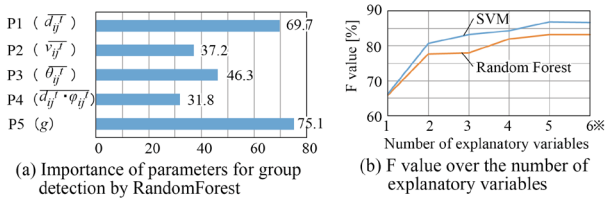

(a) Importance of parameters for group detection by RandomForest

(b) F value over the number of explanatory variables

※Average product of relative distance d_{ij}^t × the number of nearby people n_{ijr}^t was used for the sixth explanatory variable.

Figure 6. Effectiveness of detection parameters.

Figure 6(b) shows how the F values varied with the number of explanatory variables employed during machine learning. All the detection parameters were useful, and up to a point, as the number of explanatory variables increased, so did the detection accuracy. However, adding 6th explanatory variable, the average product of relative distance d_{ij}^t × the number of nearby people n_{ijr}^t, did not increase the F value. This was inferred to be because adding the information of n_{ijr}^t was included in the information of the number of seconds (P5) which was coupled in the Gabriel graph. Since the pedestrian density parameters and adjacency relationships were not examined in the existing research, they can be considered newly discovered and significant group detection parameters.

6. Estimation and Validation of the Model

6.1 Parameter Estimation

People are expected to feel stress in different ways, depending on their attributes, such as whether they are patients, helpers, and hospital staff, or if they use mobility aids. Accordingly, parameter levels are adjusted to match the model attributes. The measured trajectory records (Trajectories A and B) did not incorporate attribute information, aside from the groups. Therefore, a separate measured trajectory record shown in Fig. 7 (Trajectory C), which was established by Surveys 2-1 and 2-2 in the pre-remodeled Hospital S, was examined with respect to those attributes. The attribute data for all the people entering the survey area was added to Trajectory C by the visual observation team. However, since no information was kept regarding groups, the SVM-based group detection model constructed above was employed to supplement the group data.

(a)Outline of the survey (Surveys 2-1 and 2-2)

	Survey 2-1:Behavior monitoring survey by laser scanner sensor	Survey 2-2:Survey of pedestrian attributes by visual observation
Survey date	Wednesday, October 21, 2015	
	6:50~17:00	7:30~9:30, 10:30~12:20, 14:30~15:30
Survey method	Using eight laser sensors, measure the positions of pedestrians	The entrance time and attributes of pedestrians entering the survey area were visually inspected

Attribute information is attached to trajectory data based on time and position information.
⇒Trajectory (C) [10:30〜11:30, Wed, Oct 21]

(b)Plan of the survey area (266 m²)

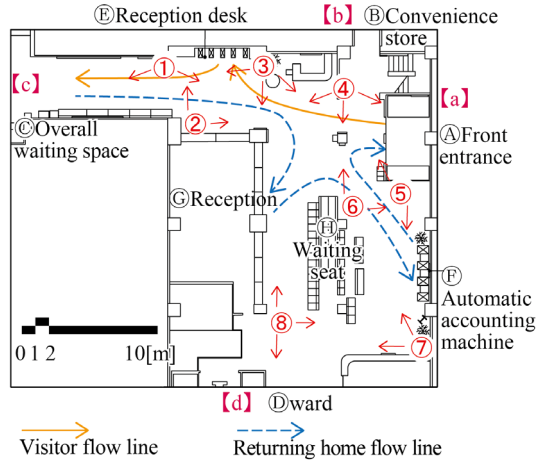

Figure 7. Outline of survey at the hospital before remodeling.

After learning had been performed with the Trajectory A, 161 group pairs were detected in the Trajectory C by using the model. These results are given in Table 1. The parameters were set using the gradient method in order to minimize the average error for each of the pedestrian attributes (sex, staff member or not, need for mobility aid or not). As shown in Fig. 8, the sum of the errors between the walking trajectory predicted by the model and the actual walking trajectory was found for all pedestrians, after which the parameters were calculated that provided the lowest value for that sum divided by the total walking time for all pedestrians.

	Trajectory C	Trajectory A
Number of trajectories	1605	800
Number of group pairs	161	115

Table 1. Result of group detection by SVM

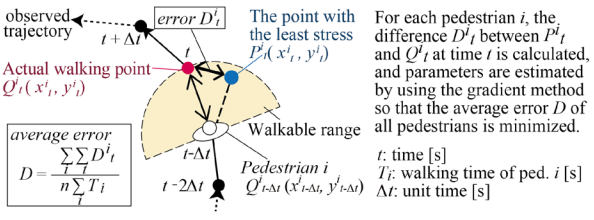

Figure 8. Definition of average error in estimation.

6.2 Interpretation of Estimated Parameters

The various ways in which people with different attributes experience psychological stress can be read from the estimated parameters. All of the aspects of Fig. 2(c) I–III are included in Model C. This is a superior model that shows variations in pedestrian behavior characteristics based on their attributes. The values for the stress types were calculated using the estimated parameters for Model C. Figure 9 shows how the stress levels for *PS*, *DS*, *OS* and *GS* were expected to vary as the relative distance increased. Based on their displayed behavioral characteristics, the results shown in Fig. 9(b) indicate that pedestrians who depend on mobility aids suffered higher destination stress, particularly in the form of the difficulties accompanying sudden direction changes.

In contrast, staff members showed lower values for all the types of stress, as shown in Fig. 9(a-d). There was little difference between the pedestrian stress suffered by staff members in regard to members of the same group and that in regard to members of another group, as shown in Fig. 9(d). This lower level of stress due to the surrounding environment was typical of staff, who constantly deal with patients and hospital visitors.

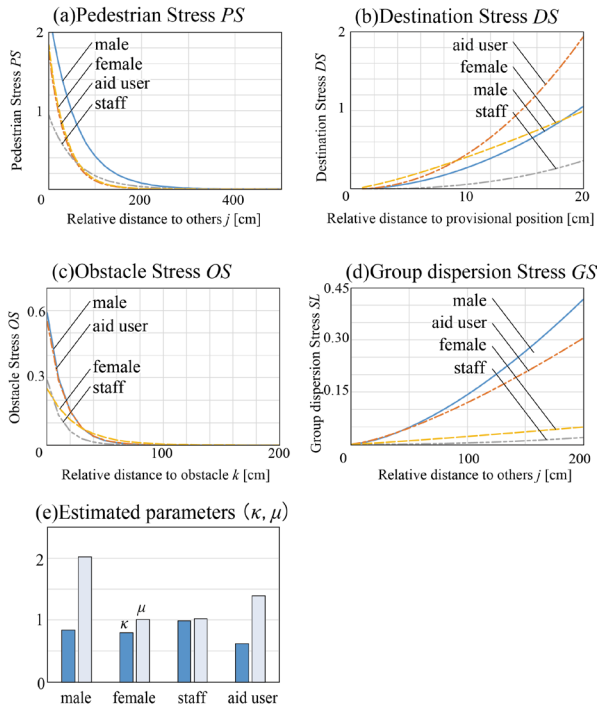

Figure 9. Estimated parameters of walking model (model C).

6.3 Pedestrian Behavior Model Validation

The validation of this pedestrian behavior model was pursued using three different approaches. (1) First, the accuracy of small spatial motions was validated. Specifically, it was verified that the direction and distance of motion from one point in time to the next had been predicted. Figure 10(a) shows the average value for the distance between the values predicted by Models A, B, and C and the actual values (average errors). They showed average errors of around 5 cm, which is considered generally good accuracy when predicting pedestrian motions. Model C, which incorporated all of the aspects described in Fig. 2(c) I–III, resulted in the lowest average error.

(2) The next step in the validation process was to verify that the behavior of single selected pedestrians was correctly expressed. Here, it was assumed that pedestrian *i* moved in accordance with Model C while all other individuals moved in accordance with the measured trajectory record (Trajectory C), and the motion of each pedestrian *i* was analyzed. The trajectory error was defined as shown in Fig. 10(b), while Fig. 10(c) presents the distribution of trajectory errors for different pedestrian attributes. These results show that the errors were within 80 cm for about 80% of the pedestrians with any given attribute. Therefore, the accuracy levels for trajectories predicted by this model were generally good.

(3) Finally, we attempted to model conditions in which multiple pedestrians maneuvered past each other in complicated conflicting patterns. Given the clock times and pedestrian entrance locations, their walking speeds, and their destinations (all drawn from Trajectory C), along with the motions of all the pedestrians present, were simulated according to Model C. Here, we focused on the group pairs detected in the previous Section and compared the trajectories predicted by the behavior simulation with the actually observed trajectories. In Fig. 11, which presents an example of the comparison results, we see that group pedestrians #285 and #286 maintained a constant distance between themselves, thus indicating that they were moving as a group. Hence, we can conclude that this simulation provided good accuracy.

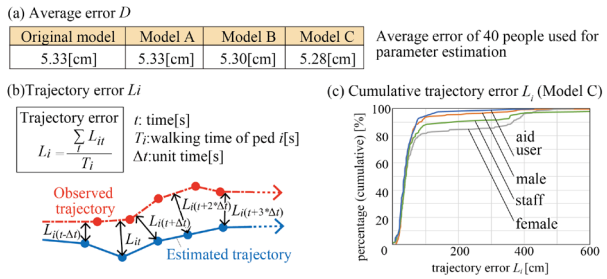

Figure 10. Validation of pedestrian behavior model.

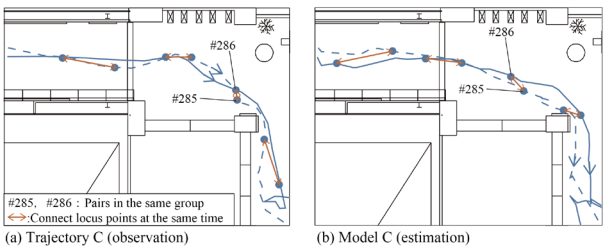

Figure 11. Observed trajectory and simulation result.

7. Evaluation of Pedestrian Space

Trajectory C and the parameters of Model C were employed to calculate the average value S_m for stress levels at each location m (on the 50 cm × 50 cm grid in the test region) and to verify the spatial distribution of S_m. The procedure for calculating S_m is shown in Fig. 12(a). Calculated spatial distributions are shown in Fig. 12(b-d). Pedestrian stress PS_m was high in locations such as near the reception counters (i) and bill paying machines (ii), where there were more people, while obstacle stress OS_m was high in locations such as walls, seating areas, and reception counters, as shown in Fig. 12(b, c). Examining the group dispersion stress GSm (Fig. 12(d)), we note that these levels are higher in locations of lower pedestrian density, where it is easier for group members to spread out (iii). The variation in each of these stress levels with time was extracted in order to obtain a slightly more detailed view; these results are shown in Fig. 12(e). It is also possible to observe the dynamic stress level changes for each individual as pedestrian experiences both

This contribution has been peer-reviewed. The double-blind peer-review was conducted on the basis of the full paper.
https://doi.org/10.5194/isprs-annals-XI-4-2026-267-2026 | © Author(s) 2026. CC BY 4.0 License.

increased dispersion stress when the other member of the group moves away and greater pedestrian stress when the group passes someone waiting in the reception area.

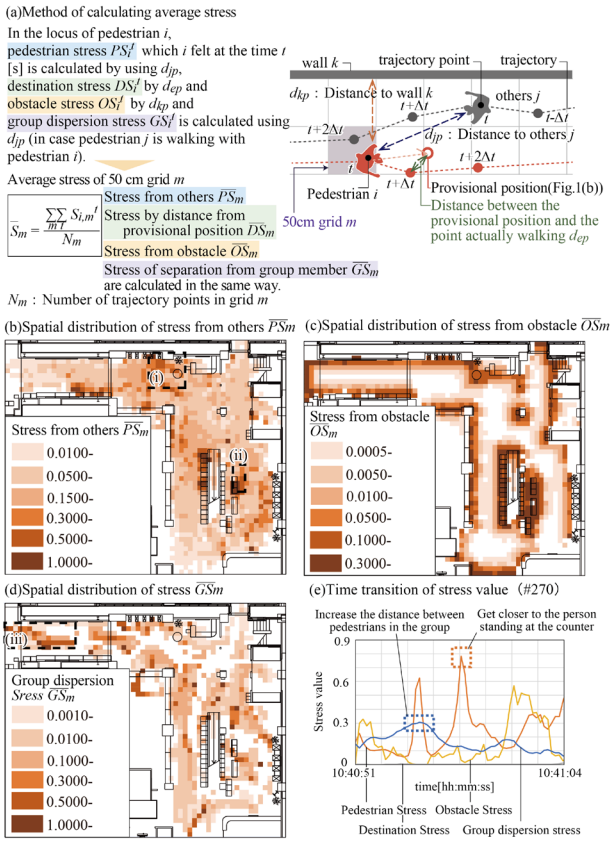

Figure 12. Pedestrian space evaluation by observed trajectory.

8. Conclusions

This study proposed a pedestrian behavior modeling framework that incorporates the existence and dynamics of pedestrian groups using high-resolution laser-based perception and machine learning techniques. By combining laser-derived pedestrian trajectories with Support Vector Machines and Random Forests, the framework enables the detection of pedestrian groups and the estimation of group-related psychological stress in real environments.

Using observational data collected in hospital atrium spaces, we demonstrated that pedestrian groups can be identified from trajectory-based adjacency relationships and that group behavior can be characterized through stress-related parameters. The proposed model explicitly represents three types of stress: individual stress experienced by group members, stress arising from dispersion within a group, and stress induced by the presence of other groups. The results showed that the model can capture differences in pedestrian attributes and behavioral characteristics, and that it provides meaningful insights into spatial patterns of stress, such as elevated stress in waiting areas and group dispersion in low-density regions.

The psychological stress estimated by the proposed model should be interpreted as a relative indicator derived from pedestrian interactions and spatial context, rather than as an absolute or directly measurable quantity. At present, no established method exists for objectively measuring walking-induced psychological stress in real pedestrian environments. Cases in which group behavior was weakly identified or partially missed highlight the limitations of the current estimation framework under certain interaction patterns and provide insight into model uncertainty.

Several limitations of the present framework suggest directions for future research. While pedestrian groups with three or more members can be represented as connected subgraphs of dyadic relations on the Gabriel graph, internal group structures such as leader–follower relationships, cohesive subgroups, or hierarchical organization are not explicitly modeled. In addition, pedestrian movement is approximated as a rational process driven by proximity-based interactions and stress-related costs, which enables interpretable modeling but does not fully capture role-based or norm-driven group behavior. Addressing these issues will require extensions toward higher-order graph representations, role-aware or norm-driven behavioral models, and temporal inference of pedestrian roles.

The use of high-resolution LiDAR is a key component of the proposed approach, as fine-scale relative positions and short-term velocity adjustments are essential for distinguishing intentional group behavior from accidental proximity. However, the limited sensing range of LiDAR sensors constrains direct application to large-scale environments. Accordingly, the proposed framework is most suitable for localized or semi-enclosed spaces such as hospital waiting halls, station concourses, or building interiors. Future work should explore sensor placement strategies, hybrid use of coarse and fine trajectory data, and hierarchical modeling approaches to extend applicability to broader environments.

By integrating group detection, stress-based behavioral modeling, and spatial evaluation within a unified framework, this study contributes a methodological foundation for pedestrian-centered analysis and design of public spaces. Further development of the proposed approach will support more comprehensive evaluation of pedestrian comfort and interaction in diverse architectural and urban contexts.

Acknowledgements

The authors would like to give their special thanks to Ms Miho Fukui (Kajima Technical Research Institute) who cooperated in our surveys at the hospital. A portion of this paper was published in Osaragi et al. (2020).

References

Borgmann, B., Hebel, M., Arens, M., Stilla, U., 2020. Pedestrian detection and tracking in sparse MLS point clouds using a neural network and voting-based approach. *ISPRS Annals of the Photogrammetry, Remote Sensing and Spatial Information Sciences*, V-2-2020, 187–194. doi.org/10.5194/isprs-annals-V-2-2020-187-2020

Chen, M., Banitaan, S., Maleki, M., Li, Y., 2022. Pedestrian group detection with k-means and DBSCAN clustering methods. *Proc. IEEE Int. Conf. on Electro Information Technology* (eIT), Mankato, MN, USA, 1–6. doi.org/10.1109/eIT53891.2022.9813918.

Ge, W., Collins, R.T., Ruback, B., 2009. Automatically detecting the small group structure of a crowd. *Proc. IEEE Workshop on Applications of Computer Vision* (WACV), Snowbird, UT, USA, 1–8. doi.org/10.1109/WACV.2009.5403123

Helbing, D., Molnár, P., 1995: Social force model for pedestrian dynamics. *Phys. Rev. E*, 51(5), 4282–4286. doi.org/10.1103/PhysRevE.51.4282

Honarvar, S., Diaz-Mercado, Y., 2024: Geometric Graph Neural Network Modeling of Human Interactions in Crowded Environments. *IFAC-PapersOnLine*, 58(28), 25-30. doi.org/10.1016/j.ifacol.2024.12.005.

Hoogendoorn, S.P., Bovy, P.H.L., 2004: Pedestrian route-choice and activity scheduling theory and models. Transportation Research Part B, 38(2), 169–190. doi.org/10.1016/S0191-2615(03)00007-9

Ma, S., Zhang, W., Noland, R.B., Andrews, C.J., Younes, H., Ann Von Hagen, L., 2025. Assessing pedestrian stress with biometric sensing and surveys. *Transportation Research Part F*: *Traffic Psychology and Behaviour*, 115, 103347. doi.org/10.1016/j.trf.2025.103347

Moussaïd et al., 2010. The walking behaviour of pedestrian social groups and its impact on crowd dynamics. PLoS ONE, 5(4), e10047. doi.org/10.1371/journal.pone.0010047

Na, J., Lee, D., Choi, H., 2023. Real-time 3D multi-pedestrian detection and tracking using 3D LiDAR point cloud for mobile robot. *ETRI Journal*, 45(4), 836-846. doi.org/10.4218/etrij.2023-0116

Nicolas, A., Hassan, F.H., 2021: Social groups in pedestrian crowds: review of their influence on the dynamics and their modelling. *Transportmetrica A*: *Transport Science*, 19(1). doi.org/10.1080/23249935.2021.1970651

Osaragi, T., 2004. Modeling of pedestrian behavior and its applications to spatial evaluation, *Proc. the Third International Joint Conference on Autonomous Agents and Multiagent Systems*, *2004*, 3, 836-843.

Osaragi, T., Homma, A., Kaneko, H., 2022. Human behavior model in public pedestrian-only space estimated using high-precision trajectory data. In: Wohlgemuth, V., Naumann, S., Behrens, G., Arndt, HK. (eds) *Advances and New Trends in Environmental Informatics*. *ENVIROINFO 2021. Progress in IS*. Springer, Cham. doi.org/10.1007/978-3-030-88063-7_10

Osaragi, T., Takeuchi, T., Kaneko, H., 2020. Pedestrian behavior model considering the presence of pedestrian groups, *Journal of Architecture and Planning* (*Transactions of AIJ*), 85(777), 2319–2328. doi.org/10.3130/aija.85.2319

Peng, X., Shan, J., 2021: Detection and tracking of pedestrians using Doppler LiDAR. *Remote Sensing*, 13(15), 2952. doi.org/10.3390/rs13152952

Sanjjamts, A., Morita, M., Enkhtogtokh, T., 2025. Real-Time Moving Flock Detection in Pedestrian Trajectories Using Sequential Deep Learning Models, arXiv:2502.15252. doi.org/10.48550/arXiv.2502.15252.

Schadschneider, A., Chowdhury, D., Nishinari, K., 2009. Stochastic transport in complex systems: From molecules to vehicles. *Elsevier*, Amsterdam. doi.org/10.1016/C2009-0-16900-3

Xiao, W., Vallet, B., Schindler, K., Paparoditis, N., 2016. Simultaneous detection and tracking of pedestrian from panoramic laser scanning data. *ISPRS Annals of the Photogrammetry, Remote Sensing and Spatial Information Sciences*, III-3, 295–302. doi.org/10.5194/isprsannals-III-3-295-2016